R-09-18

Analysis of the crystallographic signature of electron beam welds in Cu: implications for variations in etching characteristics

Patrick Trimby, Oxford Instruments Nordiska AB

June 2009

Svensk Kärnbränslehantering AB
Swedish Nuclear Fuel
and Waste Management Co

Box 250, SE-101 24 Stockholm
Phone +46 8 459 84 00

ISSN 1402-3091
SKB Rapport R-09-18

Analysis of the crystallographic signature of electron beam welds in Cu: implications for variations in etching characteristics

Patrick Trimby, Oxford Instruments Nordiska AB

June 2009

Contents

1 Introduction

The proposed design for the long term disposal of radioactive waste in Sweden involves the use of corrosion-resistant copper containers. The manufacture of these containers involves the welding of forged lids onto fabricated copper tubes; however, it has been reported (SKB report TR-02-07) that the grain sizes obtained in the lids and bottoms is much coarser than in the side walls (the tubes). The electro beam welding (EBW) of the lids onto the tubes also produces significant grain coarsening, as well as the growth of intermetallic phases at grain boundaries (SKB report TR-06-01). One of the fundamental questions regarding the suitability of these containers concerns the distribution and nature of corrosion at the lid-wall interface.

Previous studies (such as report TR-06-01) have focused on the possibility of grain boundary corrosion, and have concluded that the boundary corrosion is limited and is not likely to adversely affect the properties of the containers. However, differences in the corrosion / etching characteristics between the lid, the wall and the weld areas are observed. The cylinder wall shows reduced boundary etching compared to the weld area and the cylinder lid. This preliminary study investigates whether these differences can be explained by the crystallographic characteristics of the copper in these regions (such as the crystallographic orientation (referred to as the “texture”), the crystallographic nature of the grain boundaries and the abundance of twin boundaries).

A single sample, taken from an electron beam welded canister lid, was analysed using electron back-scattered diffraction: a summary of the results from this study and some preliminary conclusions are presented in this report.

2 Experimental methods

2.1 Electron backscatter diffraction

Electron backscatter diffraction (EBSD) has been used to characterise the microstructure of this sample. EBSD is a scanning electron microscope (SEM) technique that measures automatically the crystallographic orientation of the crystal lattice at any point on the surface of the sample. The principles of EBSD are relatively simple, and have been widely documented in the scientific literature (see /1/ and references therein). A flat, polished sample is tilted to a high angle (typically 70°) in the SEM chamber, the electron beam is positioned on a spot on the surface and a diffraction pattern is produced as a result of Bragg diffraction for individual lattice planes within the target crystal. The diffraction pattern, known as an electron backscatter diffraction pattern (EBSP) is imaged using a phosphor screen and a high sensitivity digital camera (Figure 2-1). Dedicated commercial software is used to index the diffraction pattern, thereby verifying the phase and the 3-dimensional crystal lattice orientation.

The measurement process is automated, and each measurement can be completed in less than 20 m/s. For this reason the EBSD technique is typically used to map out the orientations across a large area on the sample surface by collecting 1,000's of orientation measurements from an orthogonal grid. These measurements can then be used to reconstruct a map of the microstructure.

2.2 Equipment and analysis details

The analyses reported here were carried out at two electron microscope laboratories. Initial analyses were performed at the University of Liverpool, UK, using a CamScan X500 Crystalprobe field emission gun (FEG) SEM equipped with a Hamamatsu digital detector, with subsequent analyses taking place at Stockholm University using a Philips XL30 FEG Environmental SEM equipped with a Nordlys S digital EBSD detector from Oxford Instruments HKL. Both systems used the commercial CHANNEL5 EBSD software from Oxford Instruments HKL.

The sample was polished mechanically and given a final brief polish using colloidal silica suspension. This was sufficient to give good diffraction patterns, but some of the scratches from the mechanical polishing remained. There were also a few grains that did not polish well, and gave poor quality diffraction patterns. Electropolishing would have been a more appropriate preparation technique for pure copper, but the facilities for electropolishing such a large sample were not available at these institutes.

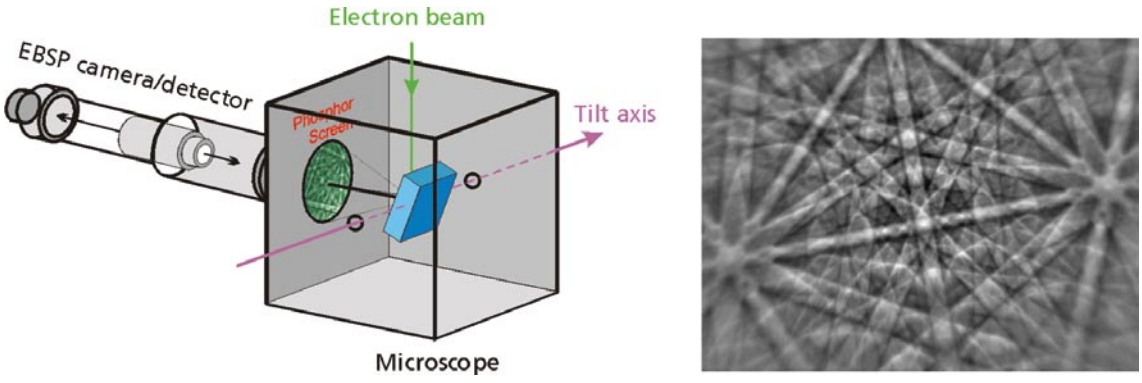

Figure 2-1. *Schematic diagram showing the basic set-up for EBSD in the SEM chamber (left), with a typical resulting diffraction pattern (right). Each band in the diffraction pattern corresponds to a lattice plane in the crystal.*

A number of automated measurements were made, covering the different areas of interest in this sample.

Figure 2-2 shows the basic structure of the sample, with the weld represented by the V shapes and the cylinder wall marked by the straight red lines at the lower right side of the sample. The sample is approximately 6 cm across.

The green box marks the approximate area covered by the EBSD analyses. These analyses were combined into a single, lower resolution transect across the whole area as well as individual, higher resolution analyses of individual zones.

These zones can be grouped into 3 categories (see Figure 2-3). Note that the sketches are not to scale.

Table 2-1. Basic information about the individual analyses. Each analysis was a montage of individual scans, stitched together to make individual datasets.

Analysis name	Grid size	Grid spacing	Number of points	Area Analysed	% indexed after filtering
Full transect	1,754 x 197	18 µm	345,538	31.6 x 3.5 mm	98.8%
Cylinder lid	912 x 492	6 µm	448,704	5.5 x 3 mm	99.9%
Weld/HAZ	1,039 x 190	18 µm	197,410	18.7 x 3.4 mm	97.2%
Cylinder wall	1,243 x 500	6 µm	621,500	7.5 x 3 mm	97.9%

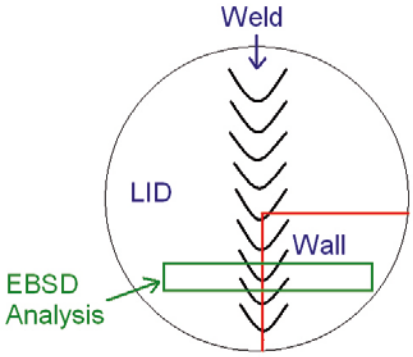

Figure 2-2.

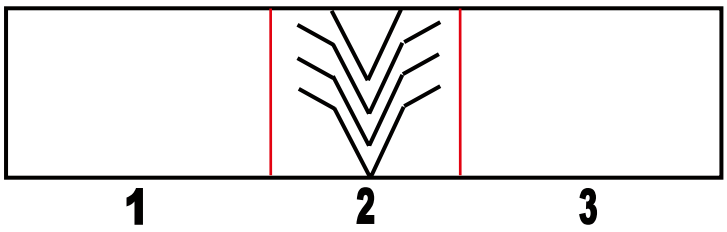

Figure 2-3. *(1) Lid. (2) Weld area with adjacent heat affected zones (HAZ). (3) Wall.*

3 Experimental results

An orientation map, reconstructed from the orientation measurements at each point, provides a summary of the microstructure of the whole transect, as shown below. The colours correspond to the crystallographic direction that is parallel to the surface normal, as shown by the triangular colour scheme. This image (Figure 3-1) provides an overview of the whole transect (nearly 32 mm across), clearly showing the coarse grained weld metal, the adjacent heat affected zones and the finer grained lid and wall material to the left and right respectively.

Although it is standard to display EBSD data in the form of orientation maps, as in the previous image, in this study orientation maps are not particularly useful. This is because there are 3 different characteristics that are likely to explain the difference in etching between the cylinder wall and the weld/HAZ and cylinder lid regions, and orientation maps do not display these characteristics effectively. The microstructural characteristics in question are:

1. The texture (i.e. the degree and nature of alignment of the crystallographic lattices in the different regions).
2. The frequency distribution of grain boundary misorientations (i.e. the change in crystallographic orientation between grains either side of a boundary).
3. The frequency of twin boundaries.

Each one of these characteristics is considered in detail in the following sections.

3.1 Texture

The texture of a sample can be calculated and displayed in a number of ways: graphically – in the form of maps showing regions with specific orientations, in pole figures – plots showing the orientation of specific crystallographic axes relative to the sample, and using orientation distribution functions (ODFs) – mathematical representations of a texture's strength and characteristics.Here ODFs are used, as they provide the most accurate method to compare the texture characteristics of the different regions in the sample.

An ODF is calculated by analysing the orientations as plotted in "Euler Space". This is a 3-dimensional space created by taking the 3 Euler angles, φ1, Φ and φ2, that are used to describe the orientation of the crystal lattice at each point, and using them as 3 orthogonal axes to define the orientation space. The densities of individual textures are calculated using a series expansion method, as described in Bunge, 1982 (reference /2/).

Figure 3-1. *Microstructure of the transect.*

Specific slices are taken through the ODF plot, and density profiles can be chosen in order to look at the strength of individual texture components (known textures that develop under specific processing conditions for particular materials). The study of ODFs is the most common way of analysing and interpreting textures in the metals processing industry, due to the historical importance of X-ray diffraction techniques.

In face centred cubic (FCC) metals, such as copper, it is convention to take slices through the ODF keeping the φ2 value constant. It is apparent from both the scattered point ODF and the calculated density ODF (Figure 3-2) that it can be difficult to determine individual textures from a 3D plot (in this case the data are taken from the cylinder wall). However, it can be seen that there are regions of high intensity in the calculated density plot, corresponding to texture components that are well developed in the cylinder wall.

In Figure 3-3, serial sections are taken through the 3D ODF for the cylinder wall (as plotted in Figure 3-2b), keeping the φ2 value constant at 5° intervals. The distribution of high density clusters can be attributed to 2 different texture components:

a) A cube texture. This is the alignment of the poles to the {100} planes with the primary sample axes (for example the rolling direction, transverse direction and normal direction – see the schematic illustration below). A cube texture creates density clusters at the corners of the 3D ODF space (see Figure 3-2b).

b) A brass/Goss texture. These 2 textures correspond to the alignment of the {011} planes, and are characterised by density clusters along the Φ=45° line.

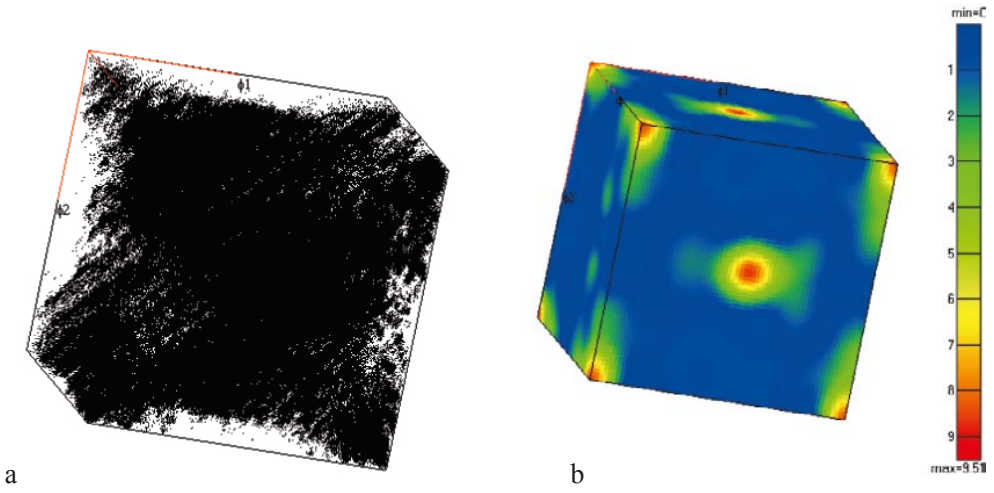

a b

Figure 3-2. *(a) Scattered points 3-D ODF plot of the orientations in the cylinder wall. Each point corresponds to a single orientation measurement. (b) 3D ODF showing the calculated densities from the orientations in the cylinder wall. The scale shows densities compared to a uniform distribution.*

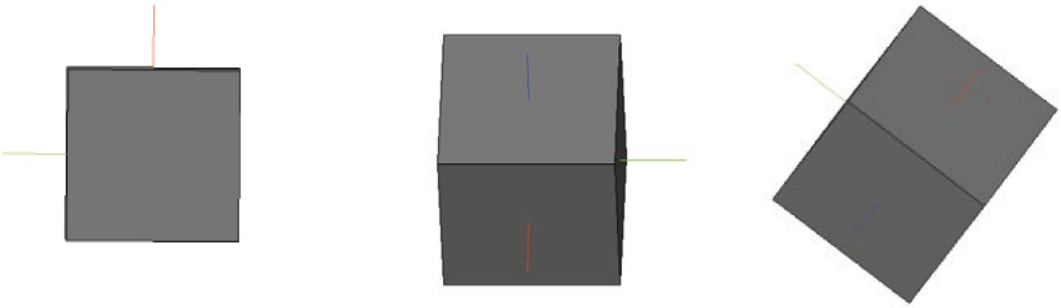

Cube Goss Brass

Figure 3-2c. *Schematic Unit Cell displays showing the orientation characteristic to the 3 texture components: Cube, Goss and Brass.*

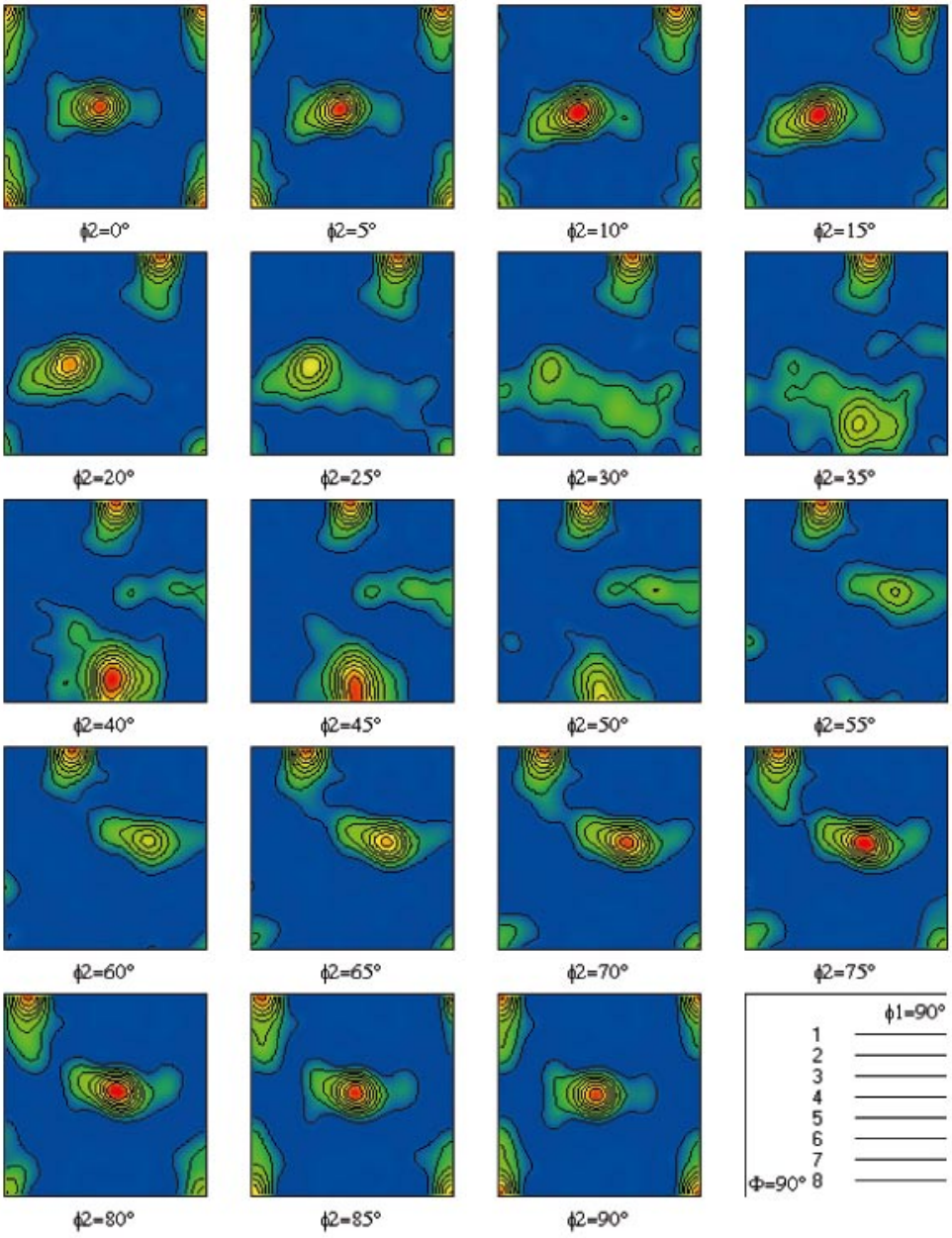

Figure 3-3. Serial sections through the calculated density ODF for the cylinder wall, keeping φ2 constant. The densities correspond to specific textures that are well developed in this region.

In order to see the relative intensities of these major texture components, a single section through the ODF with φ2=0° is all that is necessary. These have been plotted for all 3 areas in this sample, the cylinder lid, the weld/HAZ and the cylinder wall (Figures 3-4abc). It can be seen that there are significant differences in the texture between these areas: the strength of the overall texture can be expressed as a "J-index" (see reference /2/). A J-index of 1 represents a random texture, whereas a J-index of infinity represents a single crystal. The following J-index values were measured in the 3 regions in this sample:

Area	J-index
Cylinder lid	1.22
Weld/HAZ	1.96
Cylinder wall	2.91

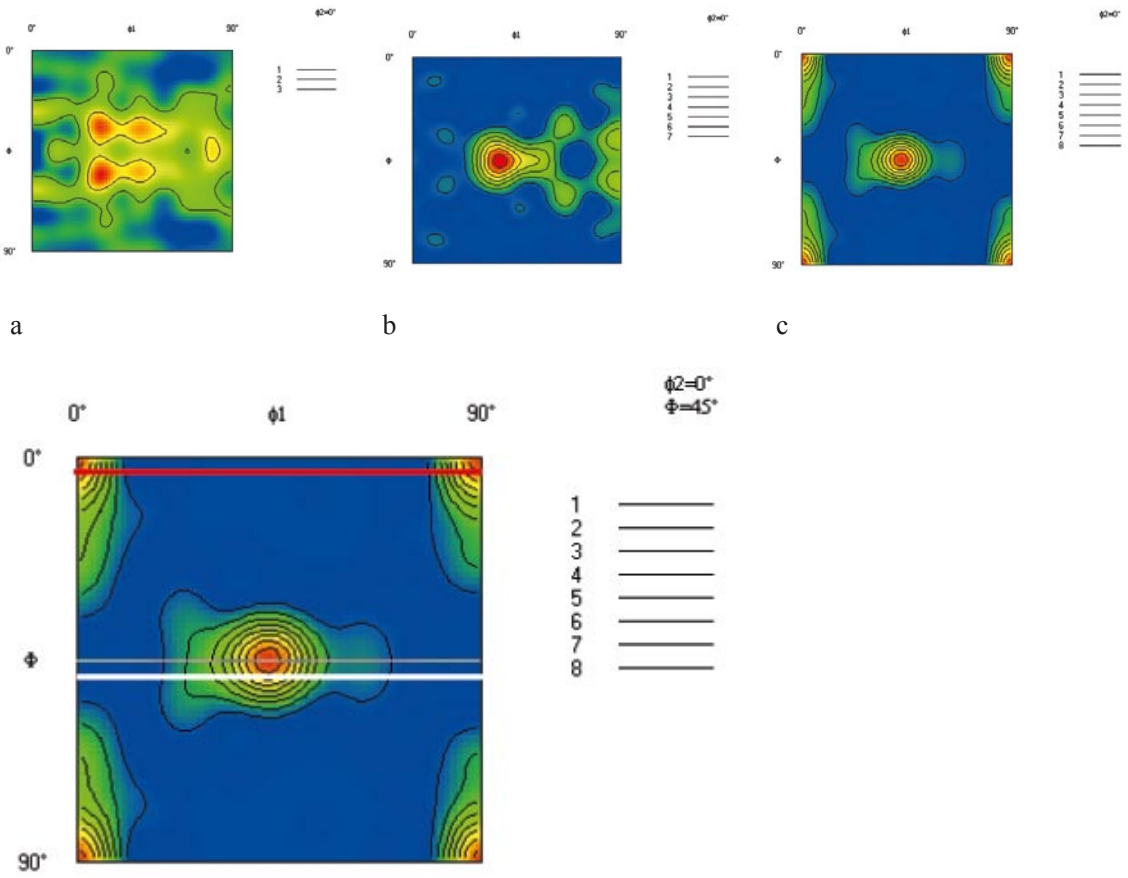

Figure 3-4. *(a) φ2=0° ODF section for the Cylinder lid. (b) φ2=0° ODF section for the weld/HAZ area. (c) φ2=0° ODF section for the Cylinder wal. (d) Highlight of the φ2=0° ODF section for the Cylinder wall, showing the density profile transects plotted in Figure 3-5. White: Φ=45° (to show the Goss and brass texture strength) and red: Φ=0° to show the cube texture strength.*

It is clear that the texture is much more strongly developed in the Cylinder wall. The differences in the texture between the 3 areas are further highlighted by density profiles along both the Φ=0° and the Φ=45° lines as shown in Figure 3-5.

The major difference between the cylinder wall and the rest of the sample is the development of a strong cube texture. In Figure 3-5 (a) it can be seen that in the cylinder wall, the cube texture component (at φ1=0° and 90°) is over 8 times stronger than would be expected in a random textured sample, whereas in the weld/HAZ and cylinder lid areas, it is less well developed than would be expected in a random textured sample.

There also exists differences in the Goss and brass texture component development (Figure 3-5b). In all areas the brass texture development (at φ1=0°) is no stronger than in a random textured sample, but the Goss texture is weakly developed in the Cylinder lid (2 times random), and strongly developed in the weld/HAZ and the Cylinder wall (7–9 times random).

An assessment of how these texture variations affect the etching characteristics is given in the Discussion section.

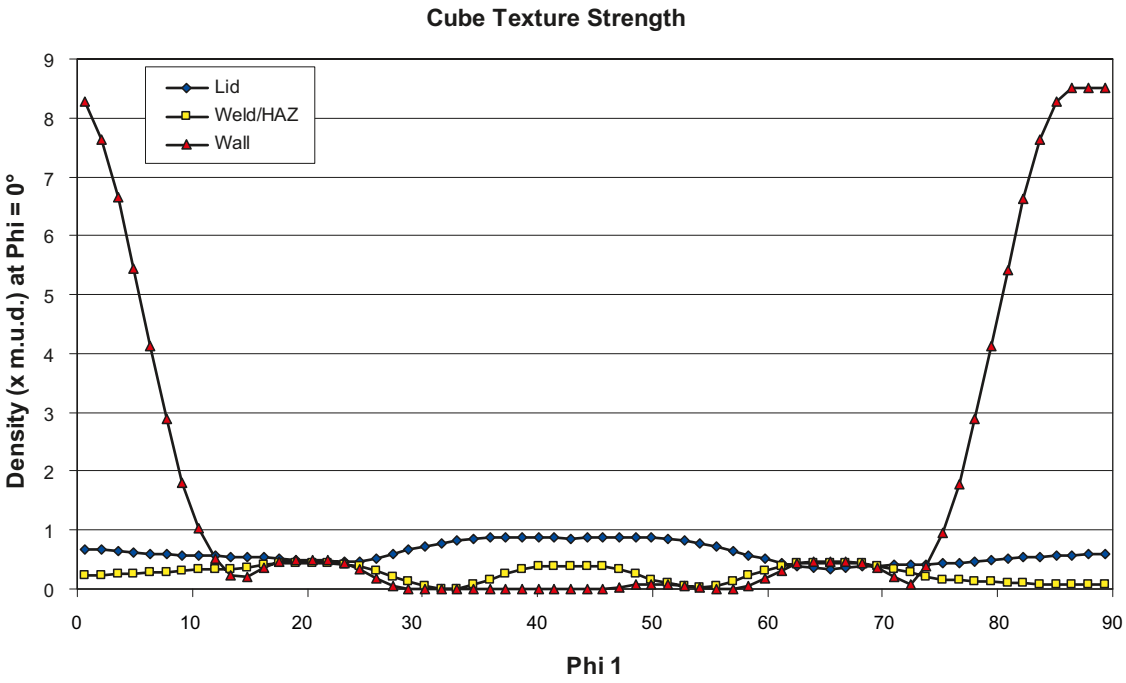

Figure 3-5a. *Comparison of the strength of the Cube texture component (along the Φ=0° line) between the lid, weld/HAZ and the wall. A cube texture produces peaks at φ1=0° and 90°.*

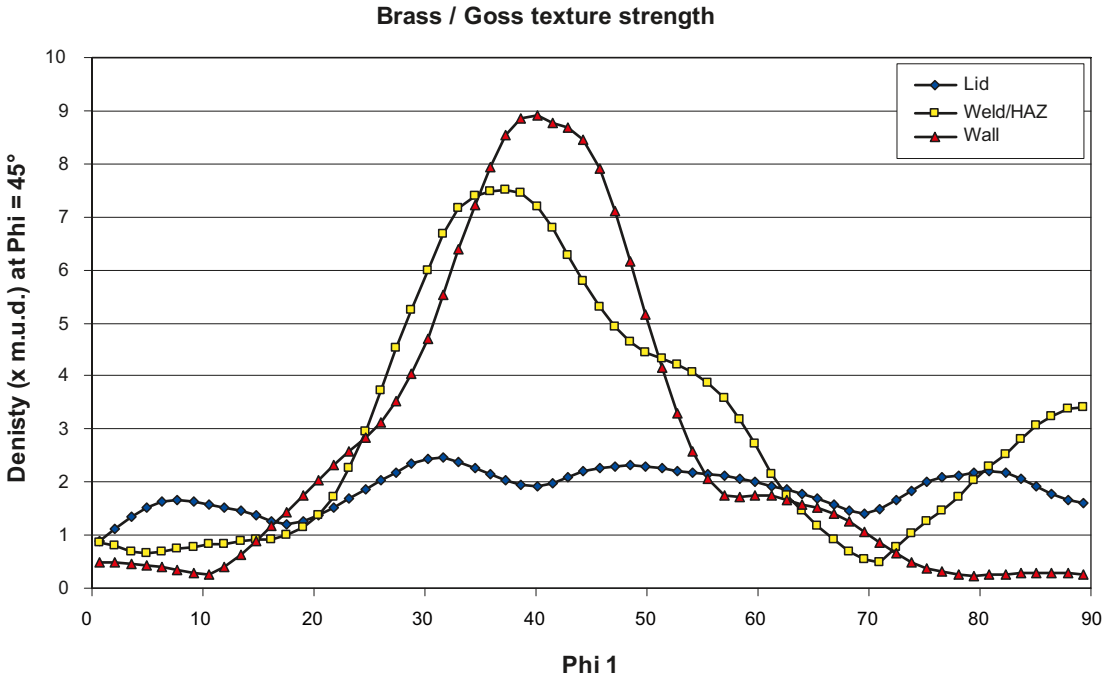

Figure 3-5b. *Comparison of the strength of the Brass and Goss texture components (along the Φ=45° line) between the lid, weld/HAZ and the wall. A Brass texture would result in a peak at φ1=0°, and a Goss texture at φ1=35°.*

3.2 Grain boundary misorientations

The EBSD technique measures the orientation of the crystal lattice at every point and, from this information, it is possible to calculate the exact change in orientation between any 2 points. This information allows us to characterise the change in orientation – or "misorientation" – across any grain boundary in the sample. It is also possible to measure the axis about which this misorientation is applied in order to rotate one crystal orientation into coincidence with another – the "rotation axis".

In many materials, a lot of the key physical properties are controlled in part by the nature of the grain boundaries. Each boundary can be expressed using 5 degrees of freedom: the boundary plane orientation (2), the misorientation angle (1) and the misorientation rotation axis (2). With EBSD we can measure 4 of the 5 parameters. The most important of these is the misorientation angle, as this can be closely related to the degree of coherence between the crystal lattices on either side. A low angle (e.g. under 10°) is indicative of a subgrain boundary, usually in the form of an array of dislocations with a degree of coherence between the 2 adjacent lattices. A high angle boundary (e.g. over 10°) is usually an incoherent grain boundary along which diffusion (and corrosion) is more likely to occur. The exceptions are twin boundaries which, although represented by high angles, have a degree of coherency across them and in which the 2 crystal lattices are linked by a specific misorientation and rotation axis. An example is the Sigma 3 annealing twin boundary, common in FCC metals (such as copper), in which the 2 lattices are related by a 60° rotation about the <111> crystal direction.

The frequency distributions of the boundary misorientations in the 3 areas is shown in Figure 3-6. The distribution is similar in all 3 areas, but there are some significant differences:

1. At low angles (< 8° misorientation) there are significantly more boundaries in the weld/HAZ zone and the wall, than in the cylinder lid. However, it must be recognised that the statistics in the weld/HAZ are distorted somewhat by the presence of several very large grains in the centre of the weld that contain low angle boundaries with 5–10° misorientations.
2. At high angles, close to 60° misorientation, there are over twice as many boundaries in the cylinder lid than in the cylinder wall or the weld/HAZ zones.
3. There appears to be a small peak present at about 38–39° misorientation in the cylinder lid that is not present in the weld/HAZ or the cylinder wall.

Some of these differences can be explained by the presence of twin boundaries, as detailed in the following section.

3.3 Twin boundary frequency

There are many different types of twin boundaries in cubic metals. The most common, the Sigma 3 annealing twin in FCC metals, has already been mentioned but there are a whole class of special boundaries referred to as "Coincident Site Lattice" (CSL) boundaries. As the name implies, the crystal lattices either side of CSL boundaries have a degree of coincidence (Sigma – Σ). The Sigma value indicates how many atoms are shared across the boundary: Sigma 3 boundaries have every 3rd atom shared, Sigma 9 every 9th and so on. Low angle boundaries (in which the distortion is accommodated entirely by dislocations) are Sigma 1 boundaries. In cubic metals, there are at least 47 different CSL boundaries that are known, although it is usually only Sigma 3 and Sigma 9 boundaries that are relatively common, and both of these are twin boundaries.

Sigma 3 CSL boundaries: 60° rotation about <111> (also referred to as annealing twins)

Sigma 9 CSL boundaries: 38.94° rotation about <110>

The EBSD technique is the perfect way to check for CSL boundaries – each CSL boundary has a specific misorientation angle and rotation axis, and these can be measured for every boundary in a particular area. The distribution of the different CSL boundaries can then be plotted in map form, for example, or in a histogram. It is also clear that the peaks in Figure 3-6 (at ~39° and 60°) referred to in the previous section correlate with the misorientations associated with Sigma 3 and Sigma 9 CSL boundaries.

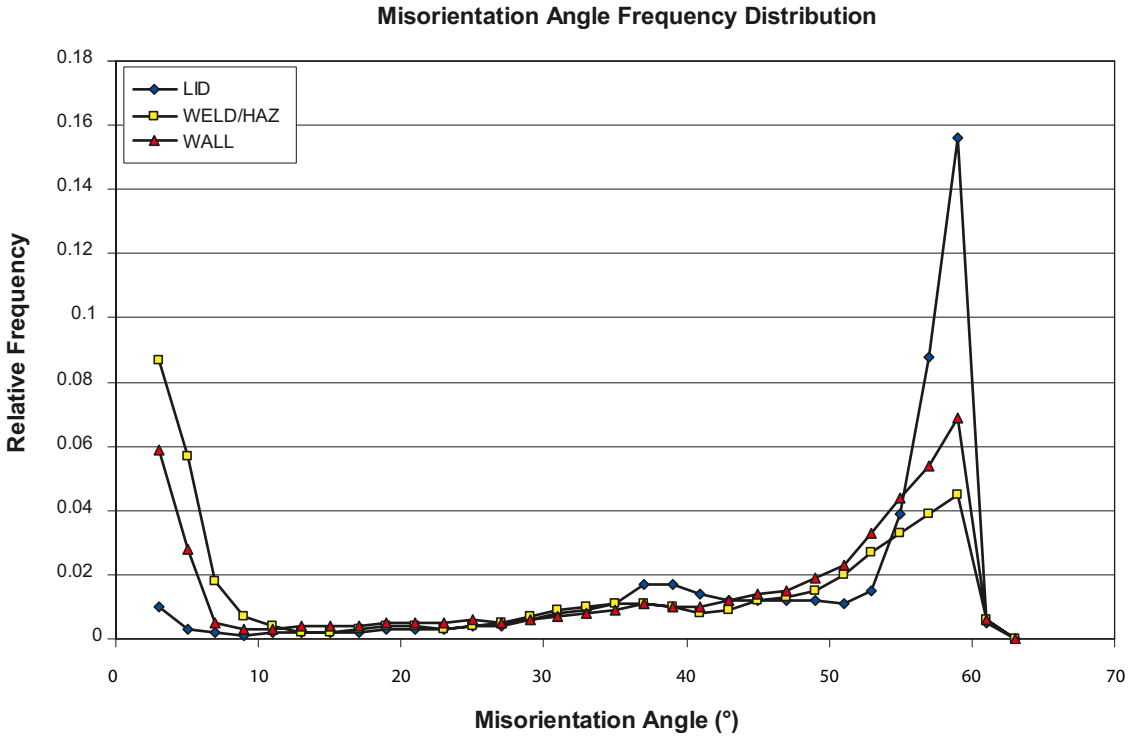

Figure 3-6. *A comparison of the misorientation angle frequency distributions for the 3 areas.*

The maps in Figure 3-7 show 2 similar sized areas in the cylinder lid and the cylinder wall, illustrating the frequency of the Sigma 3 and 9 CSL boundaries. It is clear that the Sigma 3 boundaries are extremely common in both areas (57.3% and 38.6% of all high angle boundaries in the lid and wall respectively), while the Sigma 9 boundaries are less common but still present (3.99% and 1.18% of all high angle boundaries in the lid and wall respectively). The absolute frequency of the CSL boundaries is approximately the same in the lid and wall, but the smaller grain size in the cylinder wall means that there are many more unclassified high angle boundaries in this area than in the cylinder lid – this makes the proportion of boundaries in the cylinder lid that are CSL boundaries significantly higher.

Note that the grain size in the cylinder wall is measured from the EBSD analyses to be 44.3 μm (equivalent circle diameter), compared to 89.6 μm in the cylinder lid.

Figure 3-8 compares the relative abundances of Sigma 3 and Sigma 9 CSL boundaries in the three areas, as a proportion of all high angle boundaries. It confirms that there is a significantly higher proportion of CSL boundaries in the cylinder lid than in the weld/HAZ or the cylinder wall.

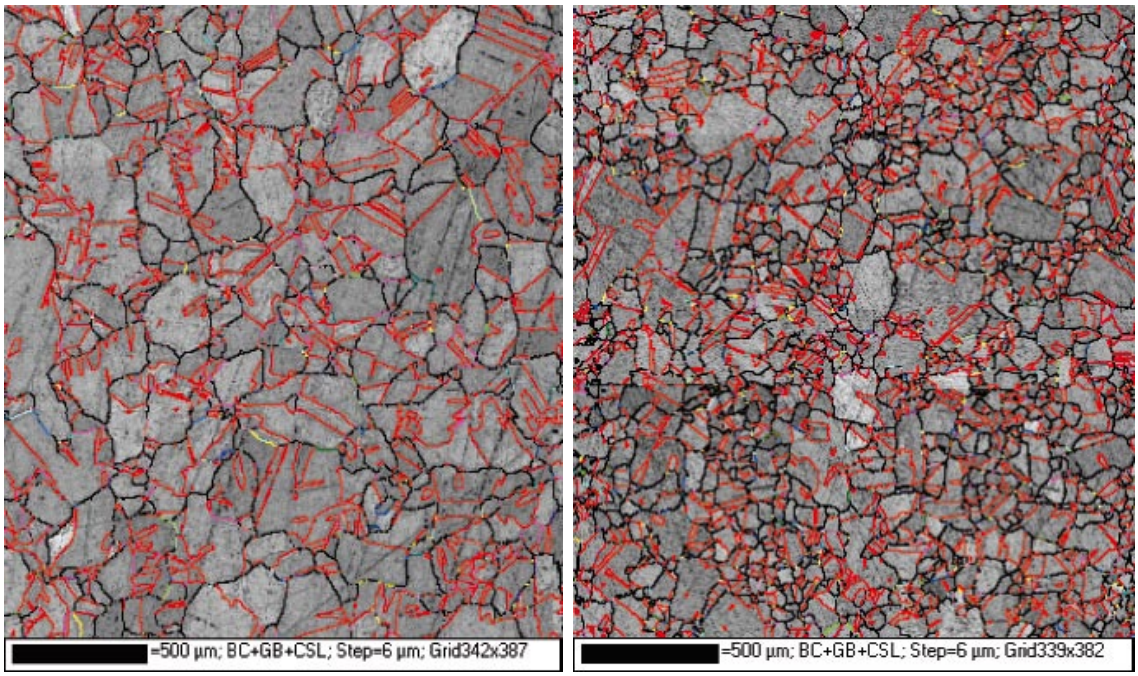

Figure 3-7. *(a) Map of part of the Cylinder lid showing the distribution of CSL boundaries. Red lines are Sigma 3 boundaries, purple lines are Sigma 9 boundaries, other colours are less common Sigma values and black lines are unclassified high angle boundarie. (b). Map of part of the Cylinder wall showing the distribution of CSL boundaries, for comparison with 7 (a). The colour scheme is the same.*

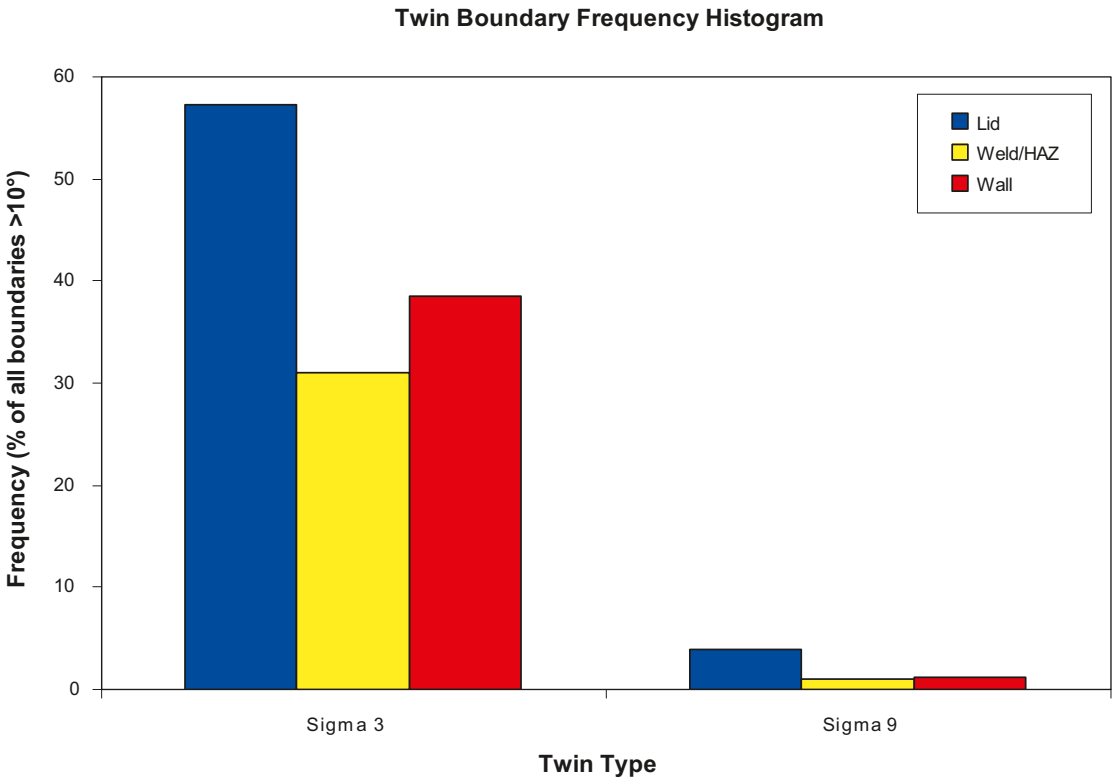

Figure 3-8. *Histogram showing the relative frequency of 2 CSL boundary types (Sigma 3 and 9) in the 3 different areas, as a proportion of all high angle boundaries over 10° misorientation.*

4 Discussion

It was proposed in the introduction that the 3 important microstructural characteristics that could influence the etching characteristics of the microstructure are the texture, the grain boundary misorientations and the abundance of twin boundaries. The results that have been presented in the previous sections illustrate that there are a number of significant differences between the microstructures in the 3 zones.

The measurements of the texture (section 3.1) show that there has been a significant texture development in the cylinder wall, compared to the cylinder lid and weld/HAZ zone. This texture is dominated by 2 components, a Cube texture and a Goss texture component. Both the Goss and the Cube textures are recrystallisation textures, formed during high temperature recrystallisation rather than deformation. Studies of the effect of temperature on the texture characteristics of pure copper (reference /3/) have shown that at temperatures of 400°C and above, dynamic recrystallisation initiates and the texture begins to be dominated by recrystallisation components, notably a strong cube texture. The following diagram (Figure 4-1) is taken from reference /3/, and shows the development of the cube texture with temperature.

The processing history of the copper used for the cylinder wall and the cylinder lid is unknown, although the texture suggests that the cylinder walls have been subjected to a higher deformation temperature than the lid. However, the effect of the development of a cube texture on the etching characteristics of the copper is unclear.

In some FCC materials, such as NaCl, it has been shown (e.g. reference /4/) that a cube texture reduced chemical etching, whereas a <111> texture (with the {111} planes parallel to the sample surface) increases the etching. This is attributed to the fact that the {111} faces have abundant sites for ionic attachment/detachment. However, in materials that oxidise easily (such as copper), it has also been proposed that the {111} faces will develop a protective oxide coat more quickly than other orientations, thus reducing the corrosion and/or etching on such oriented crystal lattices. There is also significant evidence that the more densely packed {111} lattice planes are more resistant to etching than other orientations in FCC metals.

It is therefore difficult to say at this stage with any certainty how the development of the strong cube texture in the cylinder wall will influence the etching characteristics. The difference in texture between the cylinder wall and the rest of the sample would certainly cause some differences in the etching characteristics, but exactly what differences is not known. It is clear that an in-depth review of the effect of texture on the corrosion and etching characteristics of pure copper is necessary.

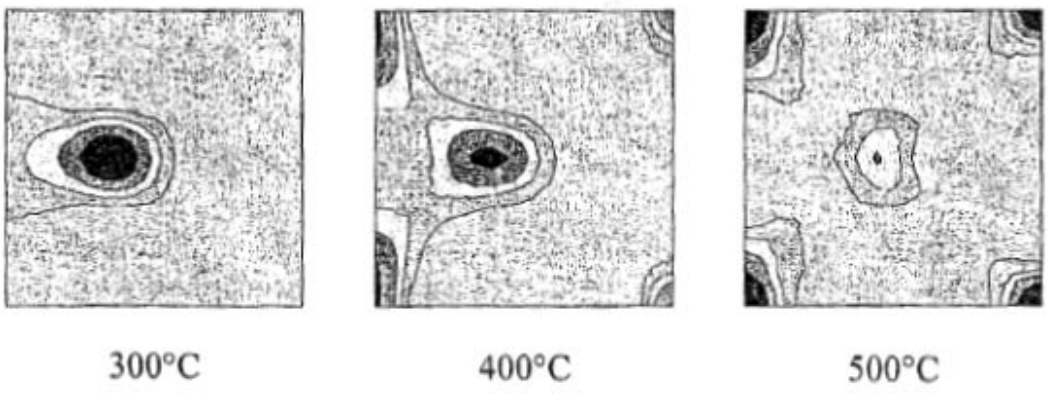

Figure 4-1. *φ_2=0° ODF sections for pure copper deformed to a true strain of 1.22.*
Figure taken from McDonald et al (2007) – reference /3/, showing the effect of temperature on the texture development in deformed, pure copper. The development of a strong cube texture (densities in the corners of the ODF) at higher temperatures is clear.

The effect of different boundary characteristics on the etching rate of a material is easier to deduce. Boundaries are zones of high etching rates, and the nature of the boundary will also be important. Boundaries with higher degrees of coherence (such as low angle boundaries and twin boundaries) will not etch so rapidly as incoherent high angle grain boundaries. The boundary maps in Figure 3-7 show that in both the cylinder wall and the lid, there are many CSL twin boundaries. However, these boundaries will be less susceptible to etching than the grain boundaries, and so we should instead look at the abundance of grain boundaries. The total length of grain boundaries per unit area is 2.3 times greater in the cylinder wall than in the cylinder lid, as a result of both the smaller grain size and the lower fraction of twin boundaries (61.3% in the lid compared to 39.8% in the wall).

The higher number of low angle boundaries in the cylinder wall (see Figure 3-5) will also increase the intragrain etching rate, although it is unclear by how much. The poor surface preparation of this sample also influences the accuracy of the low angle boundary measurement, and therefore no firm conclusions can be made on their influence.

The relatively few grains (and therefore boundaries) in the weld/HAZ zone make it statistically inappropriate to draw too many conclusions from the measurements in this area.

5 Conclusions

In this preliminary investigation using the EBSD technique, a number of key microstructural differences between the cylinder lid, the cylinder wall and the weld/HAZ zone have been measured. The most dramatic difference is in the texture of the copper crystal lattices in the different areas – a strong cube texture is developed in the cylinder wall, and this is completely absent in the cylinder lid and weld/HAZ zone. This texture difference will undoubtedly influence the etching characteristics of the different zones, but it is beyond the scope of this study to specify exactly what influence it has.

The differences in the frequencies of boundary misorientations and, more specifically, the abundance of "special" twin boundaries compared to normal high angle grain boundaries, also help to explain the differences in etching behaviour. The higher relative abundance of grain boundaries, and lower relative abundance of twin boundaries in the cylinder wall would help to explain the increased etching in this area.

It is clear that the microstructural characteristics, as measured by EBSD, can explain a number of differences in the etching rates of different parts of the copper canisters. However, it seems likely that the cause of these differences is not the welding process itself, but the primary processing of the copper used in the cylinder wall and lid. It is this primary processing that has the most impact on the texture, the grain size and the boundary characteristics, and as such the processing history of the different copper components should be investigated in greater detail.

References

/1/ **F J Humphreys, 2001.** *Review: grain and subgrain characterisation by electron backscatter diffraction*. Journal Of Materials Science **36** (2001) pp. 3833–3854.

/2/ **H J Bunge, (1982).** *Texture Analysis in Materials Science - Mathematical Methods*. Butterworths, London.

/3/ **D T McDonald, F J Humphreys, P S Bate, 2007.** *Microstructure and Texture of Dynamically Recrystallized Copper and Copper-Tin Alloys*. Materials Science Forum Vol **550** (2007) pp. 393–398.

/4/ **P W Trimby, M R Drury, C J Spiers, 2000.** *Misorientations across etched boundaries in deformed rocksalt: a study using electron backscatter diffraction*. Journal of Structural Geology **22** (2000) pp. 81–89.

Glossary of terms

Boundary Map – a map derived from EBSD data displaying the boundaries between and within grains, often coloured according to their misorientation.

CSL boundary – Coincident Site Lattice boundary, marked by specific coincidence of the crystal lattices across the boundary. The most common CSL boundaries (Σ3, Σ9 and Σ27) are twin boundaries, whilst low angle boundaries are Σ1 boundaries.

Electron backscatter diffraction (EBSD) – the technique that produces an EBSP.

Electron backscatter pattern (EBSP) – an image consisting of relatively intense bands (Kikuchi bands) intersecting one another and overlying the normal distribution of backscattered electrons, as a result of Bragg diffraction of electrons by atomic planes in the crystal lattice.

EBSP quality map – a map, from an automated EBSD analysis, in which points are shaded according to the contrast and sharpness in the EBSPs. This provides an overview of the microstructure, such as the distribution of grains, different phases and surface features. Both the contrast of the Kikuchi bands ("Band Contrast") and the sharpness of the band edges ("Band slope") can be used to generate an EBSP quality map.

Euler angles – the three Euler angles, ϕ_1,Φ,ϕ_2, (Leonhard Euler 1775) are commonly used to describe the orientation of a crystal relative to the sample.

High angle boundary – a boundary with a high angular misorientation, typically above 10°, usually referred to as a "grain boundary".

Grain boundary – a boundary between neighbouring grains or crystallites which can also be called a high-angle boundary.

Low angle boundary – a boundary with a low angular misorientation, typically below 10° (although this depends on the material in question). See "Subgrain boundary".

Misorientation – describes the orientation difference between two grains in terms of a rotation of their crystal co-ordinate systems into coincidence.

Orientation map – this is the general term to describe a map derived from the automatic grid measurement of a microstructure. Orientation maps can display a number of features of the microstructure, as well as showing boundary properties.

Orientation distribution function (ODF) – a method of representing the texture of materials. An ODF shows calculated densities of particular orientations in Euler Space.

Pole figure – a spherical projection of crystal directions displayed in a plane, used to display textures / LPOs

Rotation axis – any boundary can be described in terms of a rotation angle (see "misorientation") about a rotation axis. Special boundaries, such as twin boundaries, have specific "axis-angle" pairs.

Subgrain boundary – a boundary within a grain that separates two subgrains. Subgrain boundaries usually have a low misorientation angle, below 10°.

Texture – the preferred orientation of the crystal lattices (i.e. grains) within a material. In geology this is sometimes referred to as the "crystallographic preferred orientation" (CPO) or "lattice preferred orientation" (LPO).

Twin boundary – a high angle boundary with a specific orientation (twin) relationship between the neighbouring grains.